Helix Dipole Movement and Conformational Variability Contribute to Allosteric GDP Release in $G\alpha_i$ Subunits[†,‡]

Anita M. Preininger,[§,||] Michael A. Funk,[§,||] William M. Oldham,[§] Scott M. Meier,[§] Christopher A. Johnston,[⊥,@] Suraj Adhikary,[#] Adam J. Kimple,[⊥] David P. Siderovski,[⊥] Heidi E. Hamm,*[,§] and Tina M. Iverson*[,§,+]

Departments of Pharmacology, Biological Sciences, and Biochemistry, Vanderbilt University Medical Center, Nashville, Tennessee 37232-6600, and Department of Pharmacology, University of North Carolina School of Medicine, Chapel Hill, North Carolina 27599-7365

Received September 30, 2008; Revised Manuscript Received February 17, 2009

ABSTRACT: Heterotrimeric G proteins ($G\alpha\beta\gamma$) transmit signals from activated G protein-coupled receptors (GPCRs) to downstream effectors through a guanine nucleotide signaling cycle. Numerous studies indicate that the carboxy-terminal α5 helix of Gα subunits participates in Gα−receptor binding, and previous EPR studies suggest this receptor-mediated interaction induces a rotation and translation of the α5 helix of the Gα subunit [Oldham, W. M., et al. (2006) *Nat. Struct. Mol. Biol. 13*, 772−777]. On the basis of this result, an engineered disulfide bond was designed to constrain the α5 helix of $G\alpha_{i1}$ into its EPR-measured receptor-associated conformation through the introduction of cysteines at position 56 in the α1 helix and position 333 in the α5 helix (I56C/Q333C $G\alpha_{i1}$). A functional mimetic of the EPR-measured α5 helix dipole movement upon receptor association was additionally created by introduction of a positive charge at the amino terminus of this helix, D328R $G\alpha_{i1}$. Both proteins exhibit a dramatically elevated level of basal nucleotide exchange. The 2.9 Å resolution crystal structure of I56C/Q333C $G\alpha_{i1}$ in complex with GDP-AlF_4^- reveals the shift of the α5 helix toward the guanine nucleotide binding site that is anticipated by EPR measurements. The structure of the I56C/Q333C $G\alpha_{i1}$ subunit further revealed altered positions for the switch regions and throughout the $G\alpha_{i1}$ subunit, accompanied by significantly elevated crystallographic temperature factors. Combined with previous evidence in the literature, the structural analysis supports the critical role of electrostatics of the α5 helix dipole and overall conformational variability during nucleotide release.

Gα subunits of heterotrimeric G proteins ($G\alpha\beta\gamma$) are members of a family of more than 100 different guanine nucleotide binding proteins identified in eukaryotic cells. These G proteins transmit signals through a guanine nucleotide signaling cycle, with the protein-bound guanine nucleotide regulating the activation state of the Gα subunit (*1*−*4*). Structural and biochemical studies of Gα and small G proteins indicate that these proteins encode the information about their activation state in the conformation of loops at the protein surface. Aptly known as the switch regions, these regions switch between conformations in response to the identity of the bound nucleotide (*5*). As a result, the binding affinities for both upstream and downstream signaling proteins are dramatically affected.

GTP-bound G proteins can readily activate downstream pathways through direct protein−protein interactions. Hydrolysis of GTP to GDP by the Gα subunit returns the protein back to its inactive, $G\beta\gamma$-bound state. The uncatalyzed rate of nucleotide exchange is slow but is dramatically enhanced by the interaction with an activated guanine nucleotide exchange factor (GEF). For small G proteins, a soluble GEF catalyzes the release of GDP, while for heterotrimeric G proteins, a seven-transmembrane helix G protein-coupled receptor (GPCR) acts as a GEF to catalyze nucleotide release.

Unlike many of the small G proteins which have a single domain and a guanine nucleotide binding site that is accessible to solvent, the guanine nucleotide in the Gα subunits of heterotrimeric G proteins is nestled tightly between a Ras-like GTPase domain and a helical domain (*6*−*11*), with no obvious exit tunnel for the nucleotide. As a result, the rate-limiting step of heterotrimeric G protein signaling is release of GDP catalyzed by an activated GPCR [R* (*12*)], which physiologically requires the formation of a transient $G\alpha\beta\gamma$−R* complex. The structure determination of R* in complex with its cognate $G\alpha\beta\gamma$ heterotrimer in the nucle-

[†] This work was supported by Pilot Project funds from the Vanderbilt Institute for Chemical Biology and a Young Investigator award from NARSAD to T.M.I., NIH Grant EY06062 to H.E.H., NIH Fellowship F30 MH074266 to A.J.K., and NIH Grant GM082892 to D.P.S.

[‡] The atomic coordinates and structure factors for $G\alpha_{i1}$ I56C/Q333C (entry 3D7M) have been deposited in the Protein Data Bank.

* To whom correspondence should be addressed. H.E.H.: fax, (615) 343-1084; phone, (615) 343-3533; e-mail, heidi.hamm@vanderbilt.edu. T.M.I.: fax, (615) 343-6532; phone, (615) 322-7817; e-mail, tina.iverson@vanderbilt.edu.

[§] Department of Pharmacology, Vanderbilt University Medical Center.

[||] These authors contributed equally to this work.

[⊥] University of North Carolina School of Medicine.

[@] Present address: Institute of Molecular Biology, University of Oregon, Eugene, OR 97403.

[#] Department of Biological Sciences, Vanderbilt University Medical Center.

[+] Department of Biochemistry, Vanderbilt University Medical Center.

10.1021/bi801853a CCC: $40.75
Published on Web 02/17/2009

otide-free state would provide the most accurate information about the mechanism of nucleotide exchange for this system. Since current experimental limitations make this a daunting undertaking, the investigation of R*-catalyzed nucleotide exchange in G proteins has used alternative, low-resolution techniques. Many of the experiments have pointed to methods that can be used to stabilize Gα in its R*-bound conformation and provide new avenues for revealing mechanisms of nucleotide exchange in Gα.

The first hints of the mechanism of activation of Gα subunits by GPCRs came through mapping of the binding interface of the complex. The C-terminus of Gα subunits has long been known to interact with activated GPCRs. As early as the late 1980s, screening of Gα-derived peptides revealed that peptides corresponding to the C-terminal α5 helix of Gα could bind to receptors with high affinity and mimic G protein stabilization of the active state of the receptor (*13*−*15*). Later studies employed photoactivatable cross-linkers to show that light-activated rhodopsin could cross-link to the C-terminus of $G\alpha_t$ (*16*). The use of chemical cross-linkers confirmed the binding of the receptor to the C-terminal residues of the Gα subunit (*17*) and, additionally, identified residues within the amino terminus of $G\alpha_t$ that cross-linked to activated rhodopsin. Mapping of the receptor−G protein interaction using peptides corresponding to the cytoplasmic domain of the dopamine D_2 receptor further verified the interaction between the receptor and the C-terminus of the Gα subunit (*18*). As a complement to the peptide studies, C-terminal truncations in both $G\alpha_i$ and $G\alpha_o$ proteins have been shown to reduce affinity for GPCR, demonstrating the importance of this region in receptor affinity (*19, 20*). The C-terminus may also be important for receptor selectivity as chimeric Gα subunits that replace C-terminal residues in one Gα subtype for another affect receptor selectivity (*21*−*23*). Further, mutations within the carboxy-terminal region of Gα subunits alter receptor−G protein coupling (*24*−*26*). A fluorescence quenching approach revealed the binding site for a peptide derived from the carboxy terminus of Gα maps to a hydrophobic region on helix VI in activated rhodopsin (*27, 28*), demonstrating the utility of such approaches to providing detailed structural information, especially in the absence of a structure of an activated GPCR−G protein complex. Excitingly, a recently determined structure of opsin in complex with a peptide derived from the C-terminus of $G\alpha_t$ revealed the specific contacts between the receptor and the last 10 amino acids of the Gα subunit (*29*).

However, the carboxy terminus is not the sole region of Gα that contacts the receptor; other studies have also implicated the α4−β6 loop (*30, 31*) and the amino terminus (*13, 17, 30, 32*−*35*). Together with the C-terminus, these regions can be mapped onto the structure of the $G\alpha_{i1}$ subunit and form a contiguous, three-dimensional surface that would be anticipated for a protein binding interface (*30, 36*) (Figure 1a).

After the receptor binds its cognate G protein, the signal is transmitted from the receptor-binding site to the nucleotide-binding pocket of the Gα subunit. Electron paramagnetic resonance (EPR) spectroscopy measurements are consistent with the R*−Gα interaction causing a rotation and translation of the α5 helix of the Gα subunit toward the base of the guanine nucleotide (*37*) (Figure 1b). The insertion of a five-

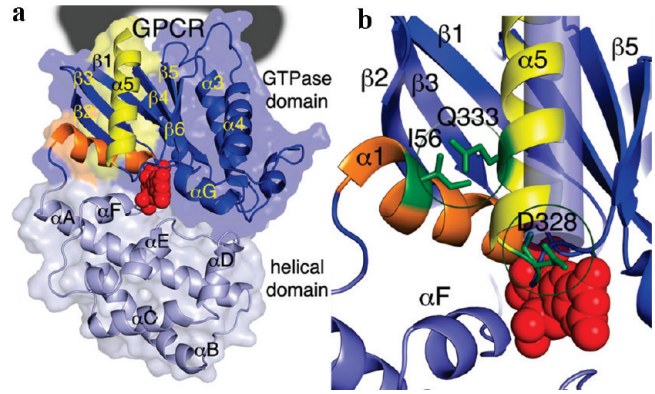

FIGURE 1: Design of the $G\alpha_{i1}$ mutants. (a) Location of the GPCR binding site on $G\alpha_{i1}$. The GTPase domain is colored dark blue, and the helical domain is colored gray. The α5 helix is highlighted in yellow; the α1 helix is colored orange, and the GDP molecule is shown in a space-filling model colored red. The location of the GPCR binding site is indicated with a black donut. The GPCR is predicted to induce a conformational change that pushes the α5 helix toward the helical domain (down in this representation). (b) Design of $G\alpha_{i1}$ mutations. Close-up view of helices α1 and α5 highlighting the locations of point mutations I56C/Q333C and D328R. The I56C/Q333C double mutation is predicted to form a disulfide bond that constrains the α5 helix into its receptor-activated conformation, which is modeled as a blue cylinder. The D328R mutation is located at the N-terminus of the α5 helix and designed to mimic the movement of the α5 helix dipole. This charge reversal mutation was designed to maximize the effect of the electrostatics.

amino acid flexible linker at the start of the C-terminal helix decouples receptor binding from the nucleotide release process (*37*), suggesting that the rigid body roto-translation of the C-terminal helix changes the conformation of the β6−α5 linker containing the conserved TCAT sequence motif, which directly contacts the guanine ring of the nucleotide, to achieve receptor-mediated allosteric nucleotide release (*38*). In addition, the structure of opsin in complex with a Gα-mimicking peptide (*29*) cannot predict the magnitude of the rigid body movement of the C-terminal α5 helix toward the GDP-binding pocket during receptor activation. However, this costructure indicates an additional conformational change of the α5 helix of Gα is required to prevent steric clash of the Gα protein with the membrane upon receptor binding. This additional conformational change was proposed as a 40° tilt of the α5 helix of the Gα subunit relative to the remainder of the G protein. A less drastic change might involve the introduction of a small bend after the C-terminus of the α5 helix. This would prevent the exposure of hydrophobic side chains along the α5 helix to solvent and is consistent with both the crystal structure and the EPR spectroscopy measurements, which shows decreased mobility for residues along the α5 helix (residues 330, 331, 334, 340, 342, 344, and 349 in a $G\alpha_i$ protein show decreased mobility) upon receptor activation (*37*).

In light of the importance of receptor-catalyzed nucleotide exchange in the Gα subunit, the changes in inter-residue distances measured by EPR spectroscopy during receptor activation (*37*) were used to develop a conceptual model of $G\alpha_{i1}$ conformation upon binding activated receptors (R*). These EPR data suggest that the roto-translation of the α5 helix plays a critical role in receptor-mediated G protein activation, which could be communicated to the nucleotide binding site via global structural effects, as well as com-

municated through specific electrostatic effects directed at the base of the α5 helix, which moves closer to the bound nucleotide upon roto-translation of the α5 helix. The roto-translation of the α5 helix indicated by EPR studies which accompany receptor activation (Figure 1b), when mapped onto existing crystal structures, results in a proximity between side chains of Gln 333 (in the α5 helix) and Ile 56, suggesting that an engineered disulfide bond between these residues could stabilize the structural changes that are present when Gα is bound to the receptor (*37*). The Gln at residue 333 is not conserved, and position 56 typically contains a hydrophobic Ile residue at this position (Leu in $G\alpha_s$).

A rigid body roto-translation of the α5 helix would also be expected to move the positive dipole of the α5 helix toward the guanine ring of the bound nucleotide upon receptor activation. To accentuate this effect, a positive charge was introduced into the base of the α5 helix of $G\alpha_{i1}$ at residue 328, a residue conserved among $G\alpha_i$ family members [D328R $G\alpha_{i1}$ (Figure 1b)]. This residue is next to the TCAT motif involved in nucleotide binding (residues 324−327). The I56C/Q333C $G\alpha_{i1}$ and the D328R $G\alpha_{i1}$ proteins (as well as other mutant proteins for control experiments) were constructed; the proteins were expressed at levels similar to that of wild-type $G\alpha_{i1}$ and could be purified using similar protocols.

EXPERIMENTAL PROCEDURES

Construction, Expression, and Purification of Rat $G\alpha_{i1}$ Mutant Proteins. $G\alpha_{i1}$ mutants were created using the QuikChange site-directed mutagenesis kit (Stratagene). The I56C/Q333C double mutant used primers 5′-AAGCAGATGAAAATTTGTCACGAGGCTGGC (I56C forward), 5′-GCCAGCCTCG-TGACAAATTTTCATCTGCTT (I56C reverse), 5′-ACGAAGAATGTGTGTTTTGTGTTCGATGCT (Q333C forward), and 5′-AGCATCGAACACAAAACACACATTCTTCGT (Q333C reverse). The D328R mutant used primers 5′-TTCACTTGCGCCACGCGCACGAAGAATGTGCAG (forward) and 5′-CTGCACATTCTTCGTGCGCGTGGCGCAAGTGAA (reverse), the D328A mutant 5′-CACTTCACTTGCGCCACGGCTACGAAGAATGTGCAG-3′ (forward) and 5′-CTGCACATTCTTCGTAGCCGTGGCGCAAGTGAAGTG-3′ (reverse), the D328N mutant 5′-CACTTCACTTGCGCCACGAATACGAAGAATGTGCAG-3′ (forward) and 5′-CTGCACATTCTTCGTATTCGTGGCGCAAGTGAAGTG-3′ (reverse), and the K330D mutant 5′-CTTGCGCCACGGATACGGATAATGTGCAGTTTGTG-3′ (forward) 5′-CACAAACTGCACATTATCCGTATCCGTGGCGCAAG-3′ (reverse). All constructs contain an internal hexahistidine affinity tag inserted between residue 119 and residue 120 in the helical domain (*39*). Proteins were expressed and purified as described previously (*39*).

Nucleotide Exchange of GDP As Measured by Intrinsic Tryptophan Fluorescence. The basal rate of GTPγS binding was determined by monitoring the relative increase in the intrinsic fluorescence ($\lambda_{ex} = 300$ nm, and $\lambda_{em} = 345$ nm) on a Varian Cary Eclipse fluorescence spectrophotometer of 500 nM wild-type or mutant $G\alpha_{i1}$ subunits in 10 mM MOPS (pH 7.2), 130 mM NaCl, and 2 mM $MgCl_2$ for 40 min at 21 °C after the addition of 10 μM GTPγS (*37*). Receptor-catalyzed exchange was performed on Gα subunits reconstituted with $G\beta_1\gamma_1$ (500 nM each) in the presence of 500 nM light-activated rhodopsin from urea-washed rod outer segments (ROS). Data were an average of three independent experiments and were normalized to the baseline (0%) and the fluorescence maximum (100%). The exchange rate was determined by fitting the data to an exponential association curve using Prism 4.0 (GraphPad Software).

Nucleotide Exchange of GDP and GDP-AlF_4^- As Measured by BODIPY-GTPγS Fluorescence. Basal nucleotide exchange was assessed as the fold increase in emission of 1 μM BODIPY-GTPγS ($\lambda_{ex} = 490$ nm, and $\lambda_{em} = 515$ nm) in buffer containing 50 mM Tris, 100 mM NaCl, 1 mM $MgCl_2$, and 10 μM GDP (pH 7.5) at 21 °C, in the presence and absence of 75 μM AlF_4^- before and after the addition of $G\alpha_{i1}$ subunits (200 nM) to the cuvette containing BODIPY-GTPγS.

Rhodopsin Binding Assay and Metarhodopsin II Stabilization. The ability of labeled Gα subunits to bind rhodopsin in urea-washed ROS membranes was assessed as described previously (*35*). $G\alpha_{i1}$ (5 μM) with Gβγ (10 μM) and rhodopsin (50 μM) in a buffer containing 50 mM Tris (pH 8.0), 100 mM NaCl, and 1 mM $MgCl_2$ were incubated in the dark, after light activation, and after light activation with the addition of GTPγS (100 μM) for a 30 min incubation at 4 °C. Membranes were separated by centrifugation at 20000*g* for 1 h, and the supernatants were removed from pellets. For the dark fraction, the reaction mixture was protected from light during centrifugation, and supernatant was removed in dim red light. The isolated fractions were boiled, visualized via Coomassie-stained SDS−PAGE, and quantified by densitometry using a Bio-Rad Multimager (*37*) by comparison of the amount of 37 kDa Gα in either the pellet or the supernatant to the total amount of Gα subunits in both fractions, and expressed as a percent of the total. Data are the average of three independent experiments. Stabilization of metarhodopsin II by increasing the concentration of Gα proteins (as detailed in Figure 2 of the Supporting Information) was performed essentially as described in ref *40* using an Olis DW2000 spectrophotometer before and after light activation of rhodopsin−G protein complexes.

Crystallization, Data Collection, Structure Determination, and Refinement. Purified wild-type and I56C/Q333C $G\alpha_{i1}$ were exchanged into crystallization buffer [20 mM HEPES (pH 8.0), 1 mM EDTA, 10 mM $MgCl_2$, 20 μM GDP, 16 mM NaF, and 40 μM $AlCl_3$] and concentrated to 10 mg/mL prior to crystallization. Crystals of the $G\alpha_{i1}$ I56C/Q333C double mutant were grown at 18 °C by the hanging drop vapor diffusion method using 2 μL of 10 mg/mL protein and 2 μL of reservoir solution [16% PEG 3350, 240 mM $Li(CH_3COO)$, 0.1 M bis-Tris (pH 6.5), and 10 mM $SrCl_2$]. Oxidizing agents were not added to the protein solution, and inclusion of DTT or β-mercaptoethanol inhibited crystal growth. For accurate comparison, crystals of wild-type $G\alpha_{i1}$ with a lipid modification were grown in the same space group using a modified reservoir solution containing 12% PEG 3350, 0.1 M $Ca(CH_3COO)_2$, and 0.1 M bis-Tris (pH 6.5). Crystals formed within 3 days and belong to tetragonal space group $P4_32_12$ with the following unit cell dimensions: $a = b = 79.7$ Å, $c = 114.5$ Å, and $\alpha = \beta = \gamma = 90°$. Crystals were cryocooled in reservoir solution containing 25% glycerol. Data for the I56C/Q333C $G\alpha_{i1}$ subunit were collected at 93 K at wavelengths of 1.0 and 1.77 Å (Table

Table 1: Data Collection, Phasing, and Refinement Statistics[a]

	I56C/Q333C	anomalous SI56C/Q333C	wild type
wavelength (Å)	1.0	1.77	0.98
resolution (Å)	2.9	3.5	3.0 (3.11−3.0)
completeness	96.8(80.6)	100.0 (100.0)	91.4 (92.6)
I/σ	20.5(1.9)	62.9 (1.8)	18.1 (3.6)
R_{sym}[b]	0.05(0.30)	0.090 (0.30)	0.08 (0.38)
figure of merit	−	0.32 (17 sites)	−
model refinement statistics			
R_{cryst}[c]	0.249		
R_{free}[c]	0.293		
rmsd for bonds (Å)	0.016		
rmsd for angles (deg)	1.7		

[a] Crystallographic data collection, phasing, and refinement statistics. Values in parentheses indicate statistics for the highest-resolution shell. [b] $R_{sym} = \sum|I_i - \langle I\rangle|/\sum I_i$, where I is the intensity, "I" is the ith measurement, and $\langle I\rangle$ is the weighted mean of I. [c] R_{cryst} and $R_{free} = \sum||F_{obs}| - |F_{calc}||/\sum F_{obs}$.

1) at Advanced Photon Source IMCA-CAT beamline 17-ID on an ADSC CCD detector. Data for the wild-type protein were collected at Advanced Photon Source LS-CAT ID-21-F at 93 K using a wavelength of 0.98 Å on a MAR CCD detector. Data were processed using the HKL (*41*) and CCP4 (*42*) suites of programs. Initial phases were calculated by molecular replacement using PHASER (*43*) using wild-type GDP-AlF_4^--bound $G\alpha_{i1}$ as the search model [Protein Data Bank (PDB) entry 1GFI (*6*)]. Sulfur-SAD phases resulting in a figure of merit of 0.32 were determined using SHARP (*44*). The molecular replacement and S-SAD phases were combined using SIGMAA (*42*). Model building was performed in O (*45*), and refinement was performed in CNS (*46*), REFMAC (*42, 47*), and PHENIX (*48*).

Structural Analyses. All structural comparisons of the GDP-AlF_4^--bound I56C/Q333C $G\alpha_{i1}$ subunit structure were performed against the wild-type protein crystallized in a binary complex with GDP-AlF_4^- in both the same space group with the same crystallographic packing ($P4_32_12$) and space group $P3_221$ (PDB entry 1GFI). Root-mean-square deviations (rmsd) of C_α positions were calculated in O (*45*), and temperature factors were calculated in CNS (*46*). Figures and movies were made using PyMOL (DeLano Scientific LLC) and LSQMAN (*49*).

Surface Plasmon Resonance (SPR) Biosensor Measurements. SPR binding assays were performed at 25 °C on a BIAcore 3000. N-Terminally biotinylated versions of peptides KB-752 [SRVTWYDFLMEDTKSR (*50*)] and KB-1753 [SSRGYYHGIWVGEEGRLSR (*51*)] were diluted to 0.1 μg/mL in BIA running buffer [10 mM HEPES (pH 7.4), 150 mM NaCl, 10 mM $MgCl_2$, and 0.005% NP40] and coupled to separate flow cells of streptavidin biosensor chips (Biacore SA chips; GE Healthcare) using the MANUAL INJECT command to a surface density of approximately 750 resonance units. Prior to injection, the Gα subunits were diluted to a range of final concentrations used to establish K_D in BIA running buffer containing either 100 μM GDP or 100 μM GDP, 30 μM $AlCl_3$, and 10 mM NaF; 40 μL of 10−50 μM Gα subunits was then simultaneously injected over flow cells at a rate of 10 μL/min followed by a 200 s dissociation phase. Signal from binding to a non-Gα-interacting, biotinylated peptide (C-terminal tail of mNOTCH1, PSQITHIPEAFK) was subtracted from all binding curves to correct for nonspecific binding and buffer shifts created during injection. Surfaces were regenerated between each injection with two pulses of 10 μL of regeneration buffer (500 mM NaCl and 25 mM NaOH) at a rate of 20 μL/min. Binding curves and kinetic analyses were conducted using BIAevaluation software version 3.0 and plotted using GraphPad Prism version 4.0b. Binding affinities were calculated using simultaneous association (k_a) and dissociation (k_d) rates derived from generated sensorgram curves.

RESULTS

Identification of the I56C/Q333C and D328R $G\alpha_{i1}$ Subunits as Functional Mimetics of R-Bound $G\alpha_{i1}$.* As structural and functional mimetics of the receptor-activated form of Gα, I56C/Q333C and D328R $G\alpha_{i1}$ proteins should exchange nucleotides at an accelerated rate, even in the absence of receptor, as compared to wild-type Gα subunits. To further characterize the mutant Gα subunits, the ability of each mutant to bind to activated receptors was compared to that of wild-type $G\alpha_{i1}$.

(1) Rates of Nucleotide Exchange. The first experiment to evaluate if the I56C/Q333C and D328R $G\alpha_{i1}$ subunits mimic R*-bound $G\alpha_{i1}$ was the measurement of the rate of nucleotide exchange. Rhodopsin is the cognate receptor for G_t, which is a member of the G_i family of proteins. Rhodopsin can also efficiently catalyze nucleotide exchange in $G\alpha_{i1}$ subunits (*37, 52*). Additionally, $G\alpha_{i1}$ subunits can stabilize extra metarhodopsin II formation in a dose-dependent manner (Figure 2 of the Supporting Information). These studies are consistent with a functional interaction between these $G\alpha_{i1}$ proteins and rhodopsin. The uncatalyzed rates of nucleotide exchange for the I56C/Q333C (0.013 s^{-1}) and D328R (0.018 s^{-1}) $G\alpha_{i1}$ subunits are both increased relative to that of the wild type under both uncatalyzed (0.002 s^{-1}) and rhodopsin-catalyzed (0.008 s^{-1}) conditions (Figure 2a−c and Table 2), consistent with the structural change in the I56C/Q333C $G\alpha_{i1}$ subunit and the electrostatic change in the D328R $G\alpha_{i1}$ subunit functionally mimicking receptor-bound Gα. Both mutant $G\alpha_{i1}$ subunits can associate with receptor (see section 2, below), and the addition of activated rhodopsin to either mutant $G\alpha_{i1}$ did not further enhance nucleotide exchange; this suggests that these mutant $G\alpha_{i1}$ proteins are maximally activated in the absence of R*. To ensure rates of exchange in the D328R $G\alpha_{i1}$ protein were not a nonspecific effect of mutation, we expressed control proteins D328N, D328A, and K220D $G\alpha_{i1}$. The D328N and K330D mutations did not dramatically perturb nucleotide exchange as compared to the wild type, and while the D328A mutant did exhibit increased basal exchange rates, it was not to the extent seen in either I56C/Q333C or D328R $G\alpha_{i1}$. In addition, the increases in the rates of exchange due to individual cysteine mutations in the background of a cysteine-depleted $G\alpha_{i1}$ protein (*37*) at residues 56 and 333 (Figure 3 of the Supporting Information), when added together, account for only half of the fold increase observed in the I56C/Q333C $G\alpha_{i1}$ double mutant (Figure 2). Finally, unlike that in the I56C/Q333C or D328R $G\alpha_{i1}$ proteins, nucleotide exchange in all of the control mutant $G\alpha_{i1}$ subunits was accelerated in the presence of activated receptor, as does wild-type $G\alpha_{i1}$ protein.

The structure of the complex between bound GDP and AlF_4^- in the nucleotide binding pocket of Gα has been

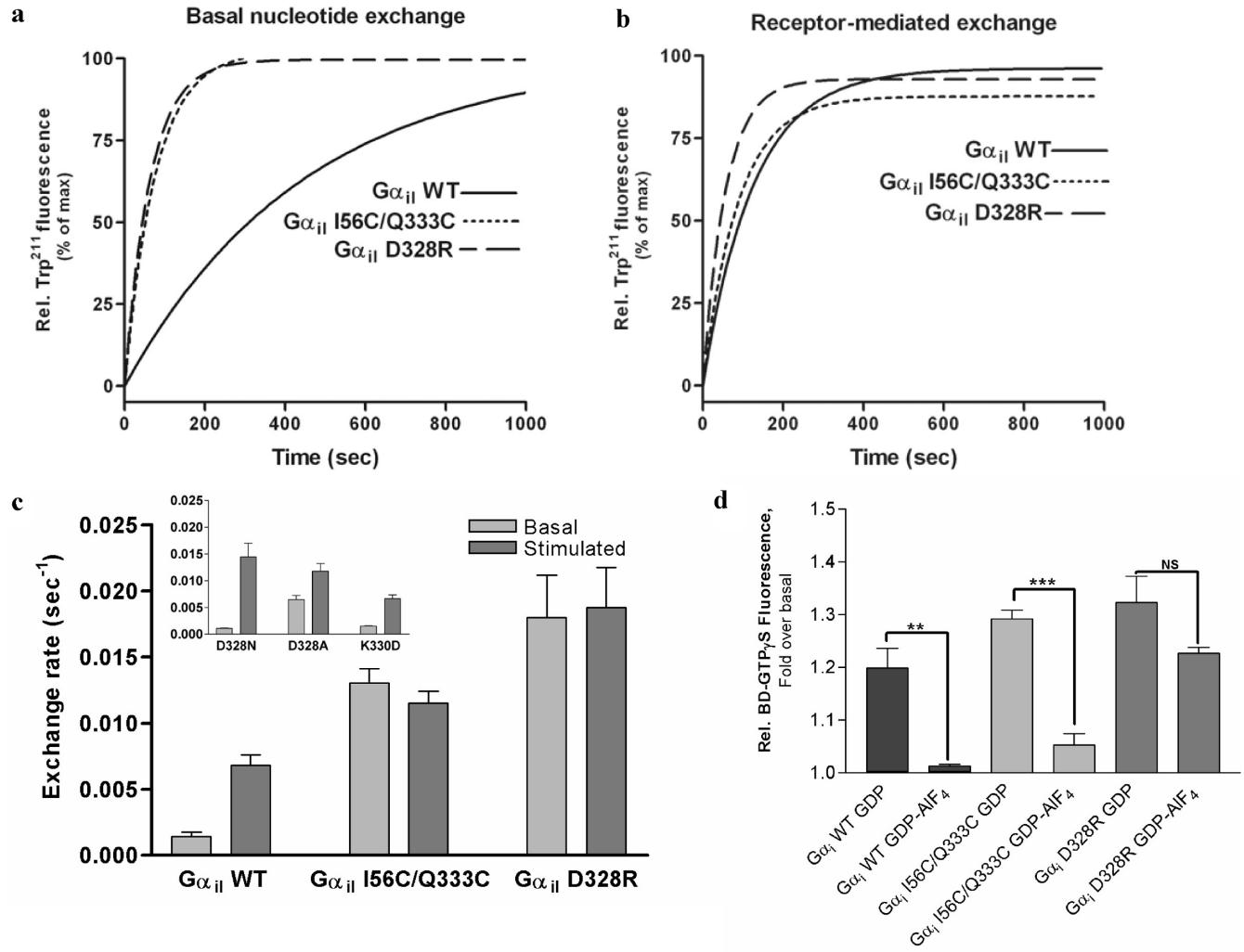

FIGURE 2: Elevated rates of basal nucleotide exchange in $G\alpha_{i1}$ mutants. (a) Basal exchange. The basal rate of GTPγS binding was determined by monitoring the relative increase in the intrinsic Trp 211 fluorescence. Basal exchange for the wild type is shown with a solid line (—), basal exchange for the I56C/Q333C double mutant with a short-dashed line (---), and basal exchange for the D328R mutant with a long-dashed line (— — —). (b) Receptor-catalyzed nucleotide exchange. Nucleotide exchange for the receptor-catalyzed wild-type and mutant $G\alpha_{i1}$ subunits was assessed by monitoring the relative increase in the intrinsic Trp 211 fluorescence performed in the presence of 500 nM rhodopsin. The addition of rhodopsin does not significantly affect the rate of nucleotide exchange in the I56C/Q333C or D328R $G\alpha_{i1}$ subunits but catalyzes a 4-fold rate enhancement for wild-type $G\alpha_{i1}$ subunits (***$p = 0.0005$). (c) Quantitation of the initial rates of basal and rhodopsin-catalyzed nucleotide exchange monitored by the relative increase in the intrinsic Trp 211 fluorescence for wild-type and mutant $G\alpha_{i1}$ subunits. (d) Basal nucleotide exchange of GDP- or GDP-AlF_4^--bound $G\alpha_{i1}$ subunits as measured by the increase in emission from BODIPY-labeled GTPγS upon addition of GDP-bound $G\alpha_{i1}$ or GDP-AlF_4^--bound $G\alpha_{i1}$ subunits. The relative increase was plotted as a percentage of basal BODIPY-GTPγS fluorescence prior to addition of Gα subunits. Data are the average of three independent experiments (**$p = 0.0027$, and ***$p = 0.0001$).

Table 2: Summary of Nucleotide Exchange Rates[a]

	basal	rhodopsin-catalyzed
I56C/Q333C $G\alpha_i$	0.013 ± 0.001	0.012 ± 0.0008
D328R $G\alpha_i$	0.018 ± 0.003	0.019 ± 0.003
wild-type $G\alpha_i$	0.0021 ± 0.0001	0.0081 ± 0.0009

[a] GDP exchange rates (s^{-1}) for wild-type, I56C/Q333C, and D328R $G\alpha_{i1}$ subunits. The exchange rate was determined by fitting the data to an exponential association equation $\Delta\lambda = \Delta\lambda_{max}(1 - e^{-kt})$. The values of k are given in $s^{-1} \pm$ SEM.

correlated to the transition state associated with GTP hydrolysis in Gα proteins. The formation of a complex between bound GDP and AlF_4^- stabilizes the bound nucleotide through additional hydrogen bonds from the nucleotide binding pocket to the GDP-AlF_4^- complex. To determine if the propensity for nucleotide release in the receptor-bound mimetics of $G\alpha_{i1}$ subunits was sufficient to overcome these stabilizing forces and release GDP-AlF_4^-, fluorescently labeled GTPγS (BODIPY-GTPγS) was used to monitor nucleotide release by measuring the increase in BODIPY-GTPγS emission after the addition of Gα subunits. GDP-AlF_4^--bound wild-type and I56C/Q333C $G\alpha_{i1}$ proteins both exhibit a decreased level of binding of BODIPY-GTPγS when compared to their GDP-bound counterparts. This suggests additional contacts mediated by binding of AlF_4^- stabilize bound GDP, reducing the level of BODIPY-GTPγS binding in wild-type and I56C/Q333C $G\alpha_{i1}$ subunits (Figure 2d). Surprisingly, both GDP-AlF_4^-- and GDP-bound D328R $G\alpha_{i1}$ subunits bound BODIPY-GTPγS to a similar extent (Figure 2d), suggesting that AlF_4^- is not sufficient to stabilize nucleotide binding in the D328R $G\alpha_{i1}$ protein. These results suggest that electrostatic perturbations at the base of the α5 helix exert distinct effects on both the affinity and duration of nucleotide binding.

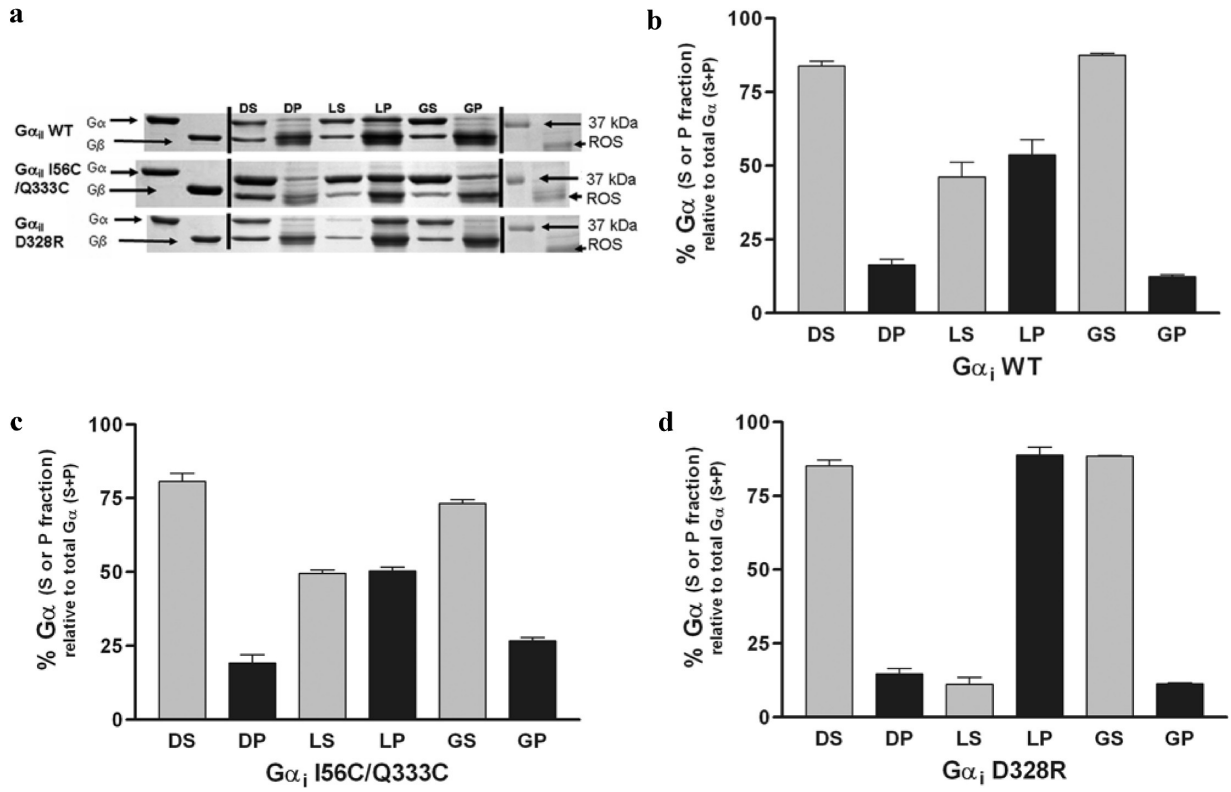

FIGURE 3: Membrane localization and rhodopsin binding of the wild-type and mutant $G\alpha_{i1}$ subunits. (a) Representative Coomassie-stained SDS−PAGE analysis of wild-type (WT) (top panel) I56C/Q333C (middle panel), and D328R (bottom panel) $G\alpha_{i1}$ subunits reconstituted with excess $G\beta\gamma$ prior to binding to ROS in the dark, light, and after light activation followed by addition of GTPγS. Abbreviations: DS, supernatant from dark sample; DP, pellet fraction from dark sample; LS, supernatant from light sample; LP, pellet from light sample; GS, supernatant from light- and GTPγS-activated sample; GP, pellet from light- and GTPγS-activated sample. (b−d) Quantitation of membrane binding. Each measurement is the average of three independent experiments. The D328R $G\alpha_{i1}$ subunit showed a significant enhancement in binding to membrane fractions upon light activation as compared to either the wild-type or the I56C/Q333C $G\alpha_{i1}$ subunit (**$p = 0.0035$ and ***$p = 0.0002$, respectively).

(2) Binding to Membrane-Bound Receptors. The ability of the GDP-G$\alpha\beta\gamma$ subunits containing either wild-type, I56C/Q333C, or D328R $G\alpha_{i1}$ to bind to rhodopsin-containing rod outer segment membranes in the dark, after light activation, and after addition of GTPγS to light-activated complexes was investigated (Figure 3). Light activation significantly enhanced the membrane association of both wild-type and I56C/Q333C $G\alpha_{i1}$ to a similar extent. Consistent with this being a more dramatic mimetic of the receptor-activated protein, the D328R $G\alpha_{i1}$ subunit had an even higher level of interaction with membrane-bound receptors after light activation than did wild-type or I56C/Q333C $G\alpha_{i1}$ proteins. As expected, subsequent addition of GTPγS dissociated the rhodopsin−G$\alpha\beta\gamma$ complex for all three $G\alpha_{i1}$ subunits, resulting in predominantly soluble GTPγS-bound $G\alpha_{i1}$ subunits.

Identification of Global Structural Changes in I56C/Q333C $G\alpha_{i1}$ by X-ray Crystallography. To determine if the physical constraint of the α5 helix by the disulfide bond in the I56C/Q333C $G\alpha_{i1}$ subunit propagated further structural changes, the crystal structure of I56C/Q333C $G\alpha_{i1}$ was determined in complex with GDP-AlF_4^- to 2.9 Å resolution (Table 1). The structure of I56C/Q333C $G\alpha_{i1}$ is similar to that of wild-type $G\alpha_{i1}$ (Figure 1a); however, the superposition of I56C/Q333C $G\alpha_{i1}$ with the wild-type protein results in a root-mean-square deviation of 0.6 Å, which is higher than would be anticipated for the introduction of two cysteines. Excitingly, significant structural changes are located in regions of the GTPase domain previously identified for their importance in receptor binding and nucleotide binding, sensing, and exchange (Table 3).

The first statistically significant movement is at the site of introduction of the two cysteines. The initial σA-weighted $2|F_o| - |F_c|$ maps of I56C/Q333C $G\alpha_{i1}$ showed clear density between Cys 56 and Cys 333, indicating the presence of a disulfide bond (Figure 4a). This disulfide bond constrains the position of the α5 helix (residues 328−345) toward the guanine nucleotide-binding site along the helical axis (Figure 4b; average C_α displacement of 0.6 Å and maximal C_α displacement of 0.8 Å over the 17-residue helix) and shifts the position of the preceding β6−α5 loop. The disulfide bond further constrains the four C-terminal residues of the α1 helix (residues 46−57) toward the α5 helix with an average displacement of 1.0 Å and a maximal displacement of 1.5 Å. This shifts positions of the C_α atoms of the α1−αA loop (residues 59−64) an average of 1.5 Å (Figure 4b). There is also a significant, albeit smaller, effect on the positions of the C_α atoms in the preceding P-loop [residues 41−45 (Figure 4c)]. In the P-loop, a conserved glycine motif allows the backbone amide nitrogens to make hydrogen bonding contacts with the nucleotide phosphates while the conserved Glu 43 orients Arg 178 to further stabilize the bound nucleotide. The C_α positions of the P-loop are shifted slightly toward the nucleotide with an average displacement of 0.65 Å and a maximum displacement of 0.8 Å; however, the hydrogen bonding interactions to phosphate and AlF_4^- are not significantly altered, and the side chains of Glu 43 and Arg 178 do not change conformation such that the latter

Table 3: Summary of Structural Features of I56C/Q333C $G\alpha_{i1}$

structural element	residues	functional role	structural change
P-loop	41−45	phosphate-binding loop highly conserved in G proteins	0.7 Å shift of G45 C_α toward the phosphates
α1 helix	44−58	Walker A motif and connection to linker/β2−β3 loop	translation toward α5 helix and nucleotide-binding pocket by 1.0 Å
α1−αA loop	59−64	linker region between GTPase and helical domains	unfolding of αA helix at the α1−αA linker loop by 1.5 Å
β2−β3 hairpin	188−197	connects α1/α5 with switch II and β1	translation toward the β1 strand by 1.3 Å; moves with α5 helix residues
β3−α4 loop	202−207	part of switch II; pulls away in GEF peptide and Gβγ-bound structures	average 0.5 Å and maximum 1.25 Å movement away from AlF_4^-
α2 helix	207−215	switch II, GEF peptide, and Gβγ binding site	unfolding and destabilization; pulls away from phosphate pocket by 0.8 Å
α4 helix	294−299	α4 helix upstream of α4−β6 loop involved in receptor interaction	average 0.9 Å movement relative to the wild type
α4−β6 loop	312−316	known receptor contact region	average 1.3 Å movement relative to the wild type
β4−α3 loop	234−238	switch III, known to move in activating peptide structure	pulls away from switch II by 0.8 Å
β6−α5 loop	324−329	TCAT motif directly interacts and stabilizes guanine ring	0.5 Å movement toward the guanine ring of C_α and side chains
α5 helix	329−345	known receptor contact and exchange mediator	translation toward nucleotide-binding pocket by 0.6 Å

remains within hydrogen bonding contact of the phosphates. While AlF_4^- binding stabilizes the I56C/Q333C $G\alpha_{i1}$ structure in a conformation similar to that observed for wild-type $G\alpha_{i1}$ under the same conditions, the subtle differences between the two structures in the P-loop indicate a propensity toward conformational adaptability in the phosphate binding region which may aid in nucleotide release. These subtle changes are detailed in Figure 4f, the rmsd plot for this structure (as compared to the wild-type protein). Figure 4f demonstrates that while subtle changes are present throughout the protein, there are particular regions which are significantly altered as compared to the wild type, including residues in the α1−αA linker region (residues 56−64), the αB helix (residues 98−102), β2 and β3 strands (residues 190−195), the switch II region (residues 215−217), and the α4−β6 loop (residues 311−314). These differences are not related to differences in space group between the two proteins, as these changes are still noted when comparing I56C/Q333C $G\alpha_{i1}$-GDP-AlF_4^- to wild-type $G\alpha_{i1}$-GDP-AlF_4^- crystallized in the same space group.

While shifts in the positions of the α5 and α1 helices (containing residues 333 and 56, respectively) and their associated connecting loops were anticipated, several additional regions of the I56C/Q333C $G\alpha_{i1}$ have unexpectedly altered positions when compared to wild-type $G\alpha_{i1}$ (Table 3 and Figure 4b−e). These regions include the β2−β3 hairpin [residues 188−197 (Figure 4b,d)], the β3−α2 loop (Figure 4d), the α2 helix [switch II, residues 202−218 (Figure 4d,e)], and the β4−α3 loop (switch III, residues 234−240). Each of these regions has previously been shown to have important functions connected with nucleotide sensing and exchange; the switch regions in particular exhibit distinct conformations in response to the identity of the bound guanine nucleotide, thereby altering the affinity of Gα for Gβγ and other binding partners.

In addition to visible changes in atomic positions, parameters such as crystallographic temperature factors provide a measure of relative mobility in crystallographic models, and these are generally used to identify regions of increased mobility in a given structure. A comparison of temperature factors between the wild-type and I56C/Q333C $G\alpha_{i1}$ proteins crystallized in the same space group and at similar resolutions (3.0 Å for the wild type and 2.9 Å for I56C/Q333C $G\alpha_{i1}$) shows an average increase of 31 $Å^2$ for I56C/Q333C $G\alpha_{i1}$ as compared to the wild type (Figure 1 of the Supporting Information). This is consistent with the I56C/Q333C $G\alpha_{i1}$ subunit having mobility and flexibility greater than those of wild-type $G\alpha_{i1}$. The increase in temperature factors is even greater in several key regions of the protein, reaching 50 $Å^2$ above the wild type in the α1 and α5 helices and the switch regions.

Verification of Structural Changes in the Switch Regions of the I56C/Q333C and D328R $G\alpha_{i1}$ Mutants by binding to Nucleotide-State Selective Peptides. The ability of wild-type, I56C/Q333C, and D328R $G\alpha_{i1}$ subunits to bind to peptides selective for the activation state of $G\alpha_i$ proteins was analyzed by surface plasmon resonance (Figure 5). Peptides KB-1753 and KB-752 discriminate between active, GDP-AlF_4^--bound and inactive, GDP-bound $G\alpha_{i1}$ subunits (*50, 51*). We found these peptides bind to wild-type and mutant $G\alpha_{i1}$ subunits with the same selectivity (Figure 5) but with different binding kinetics and affinities (Table 4). Peptide KB-752, selective for GDP-bound Gα subunits, has been shown to bind to $G\alpha_{i1}$ at the switch II region (*50*). KB-752 has an 8-fold higher affinity for GDP-bound wild-type $G\alpha_{i1}$ subunits than it does for GDP-bound I56C/Q333C $G\alpha_{i1}$ subunits, suggesting that the switch II region in GDP-bound I56C/Q333C $G\alpha_{i1}$ likely adopts a conformation different from that observed for GDP-bound wild-type $G\alpha_{i1}$ subunits. This suggests that the altered position of switch II observed in the crystal structure is also present in solution. This peptide binds to GDP-bound D328R on the order of that seen in wild-type $G\alpha_{i1}$ subunits, consistent with these proteins sharing a similar switch II geometry where the peptide binds. Conversely, GDP-AlF_4^--bound I56C/Q333C and D328R $G\alpha_{i1}$ subunits bind peptide KB-1753 [selective for activated $G\alpha_{i1}$ subunits (*51*)] with a 3−4-fold higher affinity than wild-type $G\alpha_{i1}$-GDP-AlF_4^-. This suggests that GDP-AlF_4^--bound I56C/Q333C $G\alpha_{i1}$ and D328R $G\alpha_{i1}$ subunits readily accommodate binding of the peptide selective for activated subunits.

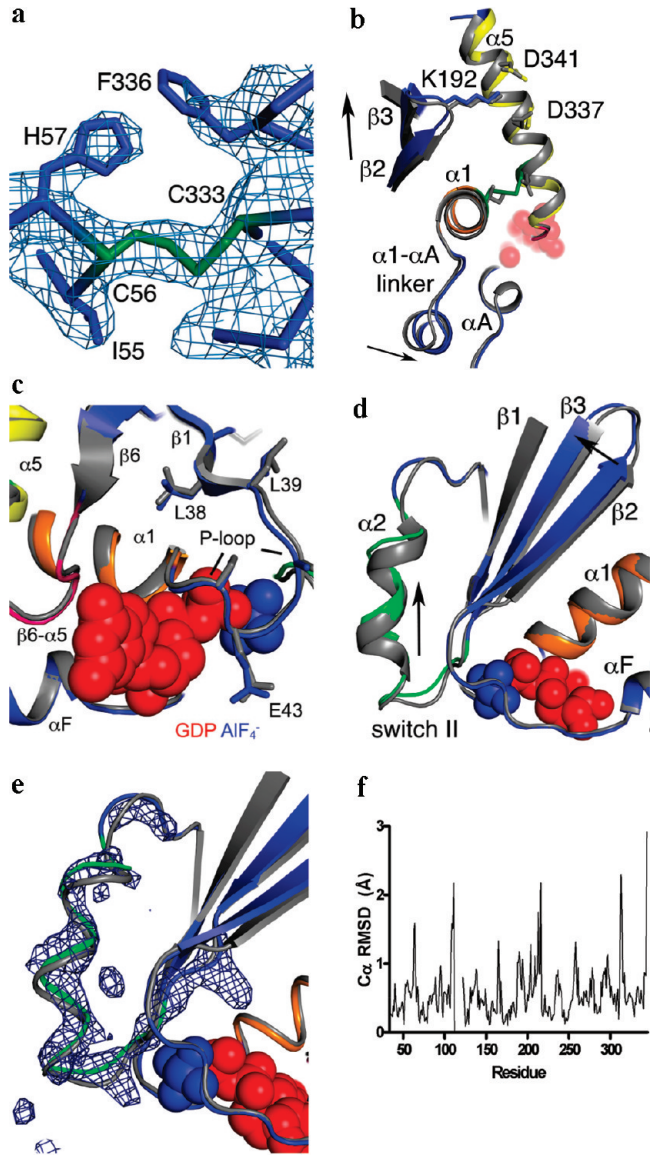

FIGURE 4: Structural changes in I56C/Q333C $G\alpha_{i1}$. All comparisons are made between the I56C/Q333C $G\alpha_{i1}$ subunit and the wild-type $G\alpha_{i1}$ subunit crystallized in complex with GDP-AlF_4^-. The coloring for panels b−d is the same as in Figure 1. (a) The $2|F_o| - |F_c|$ density (blue mesh) contoured at 1.2σ shows a connection between the side chains at positions 56 and 333 and is consistent with the formation of a disulfide bond. (b) Movement of the α5 helix, the $\beta2-\beta3$ hairpin, and the α1−αA linker that connects the GTPase (dark blue) and helical domains (cyan). (c) Movement of the P-loop. (d) Movement of the $\beta2-\beta3$ hairpin away from the α1 helix toward the $\beta1$ strand. The hairpin directly connects the second linker (residues 177−182) and switch II [residues 202−215 (light green)]. (e) The $|F_o| - |F_c|$ simulated annealing omit density calculated using CNS and contoured at 3.0σ after the removal of all atoms between residues 202 and 217 (α2 helix and switch II) highlights the shift between I56C/Q333C (blue/green) and wild-type (gray) $G\alpha_{i1}$. The GDP molecule is colored red, and the AlF_4^- is colored blue. (f) rmsd of each α-carbon atom in the I56C/Q333C $G\alpha_{i1}$ structure as compared to wild-type $G\alpha_{i1}$ (PDB entry 1GFI, selected regions overlaid in panels a−e).

DISCUSSION

In the rate-determining step of G protein signaling, activated GPCRs catalyze the release of GDP in the Gα subunit of heterotrimeric G proteins (*12*). Gα lacking bound nucleotide is unstable in solution; in vivo Gα remains bound to R* until GTP binding, which results in predominantly soluble Gα-GTP subunits, capable of activating downstream effectors. Previous studies have mapped the binding site for the receptor onto a contiguous surface of the Gα subunit (*30, 36*) (Figure 1a), identified the three-dimensional constraints underlying the interaction between the C-terminus of the Gα subunit and receptor (*29*), and characterized a rigid body movement of the α5 helix of Gα that accompanies receptor-catalyzed allosteric GDP release (*37, 53*). The latter study set the stage for this work, where the known conformational changes in the α5 helix were used as a starting point to mimic the R*-bound conformation of Gα through a disulfide bond or by replicating the movement of the α5 helix dipole.

The I56C/Q333C $G\alpha_{i1}$ Subunit Is a Structural and Functional Mimic of the R-Bound Gα Subunit.* An anticipated hallmark of an R*-bound Gα subunit is a dramatically weakened ability to bind to GDP, and a conformation predisposed to binding GTP. Enhanced nucleotide exchange in both mutant $G\alpha_{i1}$ subunits occurs in the absence of receptor and is consistent with both of these mutant subunits acting as functional mimics of the R*-bound Gα subunit. In the I56C/Q333C $G\alpha_{i1}$ variant, this is a result of structural changes that are anticipated for an R*-bound Gα subunit

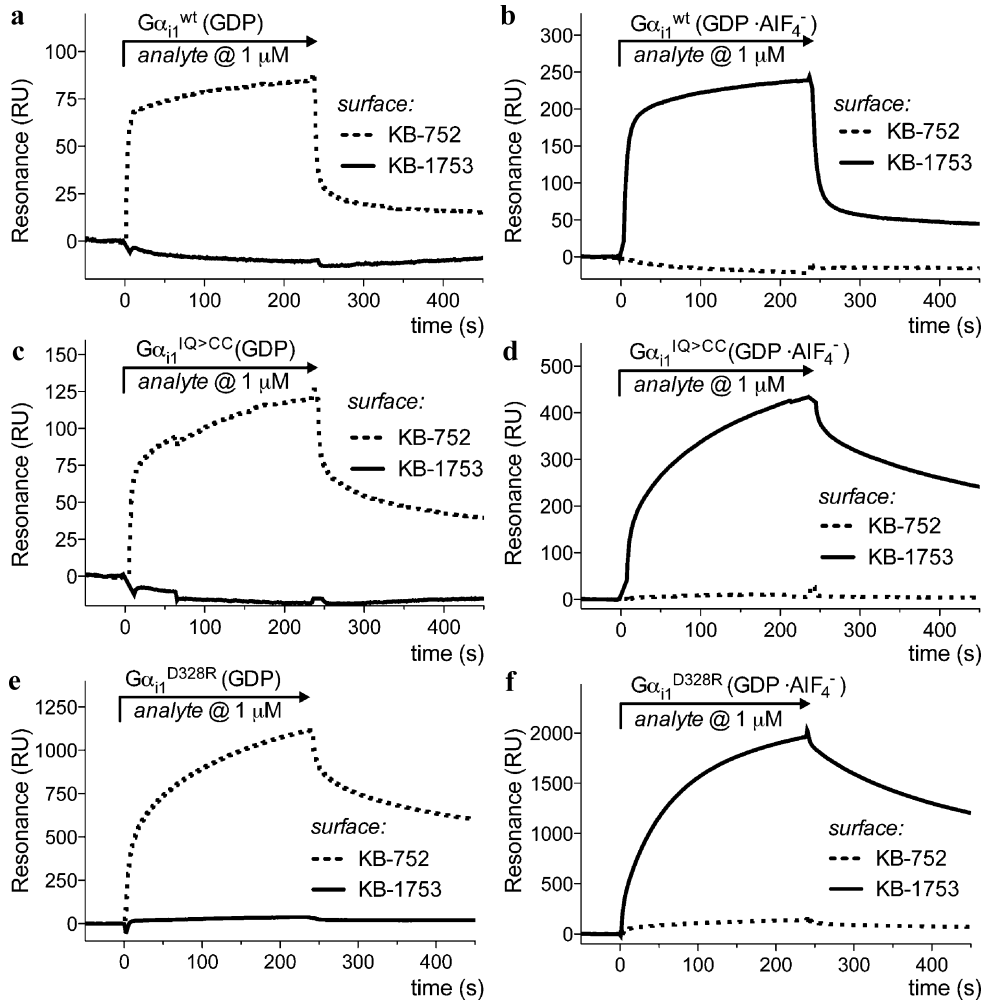

FIGURE 5: Surface plasmon resonance analysis of the binding of $G\alpha_{i1}$ subunits to nucleotide-state selective peptides. Surface plasmon resonance demonstrates peptides KB-752 and KB-1753 discriminate between the activation states of $G\alpha_{i1}$ proteins. In each graph, the dashed line represents binding of the indicated Gα subunit to immobilized peptide KB-752, selective for inactive (GDP-bound) Gα subunits, while the solid line represents binding to immobilized peptide KB-1753, selective for activated (GTP-bound) Gα subunit: (a) wild-type $G\alpha_{i1}$ in the presence of GDP, (b) wild-type $G\alpha_{i1}$ in the presence of GDP-AlF_4^-, (c) I56C/Q333C $G\alpha_{i1}$ in the presence of GDP, (d) I56C/Q333C $G\alpha_{i1}$ in the presence of GDP-AlF_4^-, (e) D328R $G\alpha_{i1}$ in the presence of GDP, and (f) D328R $G\alpha_{i1}$ in the presence of GDP-AlF_4^-.

Table 4: Comparison of k_{on}, k_{off}, and K_d Values for Wild-Type, I56C/Q333C, and D328R $G\alpha_{i1}$[a]

	k_{on} (M^{-1} s^{-1})	k_{off} (s^{-1})	K_d (μM)
KB-752 (selective for $G\alpha_i$-GDP)			
WT $G\alpha_i$-GDP	21100 ± 5800	0.06 ± 0.01	2.84 ± 0.81
I56C/Q333C $G\alpha_i$-GDP	7750 ± 250	0.22 ± 0.03	28.2 ± 2.9
D328R $G\alpha_i$-GDP	8560 ± 650	0.01 ± 0.001	1.28 ± 0.02
KB-1753 (selective for $G\alpha_i$-GDP·AlF_4)			
WT $G\alpha_i$-GDP·AlF_4^-	22900 ± 2300	0.025 ± 0.001	1.1 ± 0.1
I56C/Q333C $G\alpha_i$-GDP·AlF_4^-	16800 ± 1700	0.006 ± 0.0008	0.36 ± 0.01
D328R $G\alpha_i$-GDP·AlF_4^-	8810 ± 1390	0.003 ± 0.0004	0.26 ± 0.04

[a] Values are from an average of four trials (wild type) or two trials (I56C/Q333C and D328R).

based on previous EPR studies. Even in the presence of GDP-AlF_4^-, the crystal structure of the I56C/Q333C $G\alpha_{i1}$ subunit reveals altered positions for the switch regions, which shows switch II and switch III each have a conformation that is intermediate between those observed for the active (GTP-bound) and inactive (GDP-bound) forms of the Gα subunit.

This structure of the I56C/Q333C $G\alpha_{i1}$ subunit also exhibits increased temperature factors relative to those of wild-type structures. Crystallographic temperature factors give a relative assessment of the average displacement of any given atom in a structure, which is usually interpreted as mobility. Elevated temperature factors throughout the molecule may also reflect a greater number of substructures in the ensemble, resulting in increased frequency of conformations facilitating nucleotide release. Temperature factors are generally limited to a range of 0−100 $Å^2$ in soluble proteins, with a higher number correlating with increased motions. A 31 $Å^2$ average increase in crystallographic temperature factors is observed in I56C/Q333C $G\alpha_{i1}$ as compared to wild type crystallized in the same space group and at a similar resolution (2.9 Å for the I56C/Q333C $G\alpha_{i1}$ subunit and 3.0 Å for the wild type). These temperature factors are elevated to an even greater extent in the α1 and α5 helices and the switch I and switch II regions of I56C/Q333C $G\alpha_{i1}$, where they are an average of 50 $Å^2$ above the wild type. This suggests that the I56C/Q333C variant is more conformationally variable than the wild type, especially in these four regions. An increase in protein mobility in $G\alpha_{i1}$ proteins during nucleotide exchange has previously been noted in EPR experiments (*53*), while NMR spectra of nucleotide-free chimeric $G\alpha_t$ show significant line broadening, which has been interpreted as an increase in protein dynamics (*57*). Increased dynamics

may facilitate exit tunnel formation by moving the protein conformation into a higher-energy landscape that can more easily convert the structure of the Gα subunit into the open state.

Increased flexibility in switch II and altered P-loop conformations may also play a role in nucleotide exchange dynamics. Increased intrinsic nucleotide exchange rates of GDP-bound $G\alpha_i$ subunits compared to those of $G\alpha_t$ subunits are distinctive features of $G\alpha_i$ proteins. Another distinctive feature of $G\alpha_i$ subunits is the disorder in switch II regions, as compared to the more ordered switch II regions of $G\alpha_t$-GDP proteins. These data are consistent with the increased flexibility of this region contributing to an increased level of nucleotide exchange in $G\alpha_i$ proteins.

There are a number of statistically significant structural changes clustered in the GTPase domain of the I56C/Q333C $G\alpha_{i1}$ subunit (Figure 4f and Table 3). Many of these regions are implicated in nucleotide sensing, binding, exchange, or receptor interaction. The region linking the helical domain and GTPase domain, which in this structure shows a marked shift in position relative to the wild type, is predicted to lie some distance from the regions of Gα already known to interact with receptors, such as the C-terminus and the $\alpha4-\beta6$ loop. Consistent with an allosteric mechanism of receptor-mediated G protein activation, this region has been linked to the specificity of receptor coupling, as mutation of the residue of $G\alpha_q$ homologous to residue 61 in the linker region of $G\alpha_{i1}$ can alter the specificity of receptor coupling (*55*). The high rmsd in this region, in addition to other regions known to be involved in receptor contacts, is consistent with an overall picture of specific structural changes and overall protein flexibility, which contribute to receptor-mediated G protein activation. While these data point to factors which may play a role in nucleotide release in $G\alpha_i$ proteins, further studies are currently underway to determine which of these conformational changes contribute to GDP release and which are compensatory shifts reflecting the fact that the protein is stabilized in its GDP-AlF_4^- transition state.

Forces Contributing to Allosteric GDP Release in Gα Subunits: The D328R $G\alpha_{i1}$ Subunit Is a Functional Mimic of the R-Bound Gα Subunit.* Structural and functional characterization of the D328R $G\alpha_{i1}$ subunits suggests electrostatics from movement of the α5 helix dipole may contribute to an increased rate of nucleotide release. Shoemaker et al. (*54*) points out the stabilizing role of a negatively charged residue (such as the native Asp at position 328) at the N-terminus of an α-helix with a positively charged helix dipole (Figure 1b). The negative charge can neutralize and stabilize the positively charged helix dipole. Mutation of Asp328 to a positively charged Arg would be predicted to perturb this helix cap and deshield the amide nitrogen. Consistent with this idea, the D328R mutant exhibits a markedly increased rate of nucleotide exchange, while D328N has activity similar to that of the wild type, suggesting that the Asn can participate in stabilization of the helix dipole. Substitution of D328 with Ala would not be predicted to have the same effect, since the amide nitrogen would be deshielded. Indeed, the D328A mutant exhibits a somewhat elevated rate of nucleotide exchange compared to that of the wild type.

The use of electrostatics to initiate nucleotide release is a novel proposal for the mechanism of nucleotide exchange in G proteins. These results, combined with previous EPR studies, strongly suggest that the movement of the helix dipole during receptor binding contributes to the decreased affinity of Gα for GDP by altering the local electrostatic distribution around the nucleotide. It is possible that even subtle changes in the electric field may act to reorient the GDP as a prerequisite to nucleotide release. In the absence of stabilizing contacts between a third phosphate or AlF_4^-, even complexation with AlF_4^- cannot overcome the electrostatic perturbation of the D to R mutation, allowing GDP-AlF_4^- to be exchanged for BODIPY-GTPγS. A decreased affinity for GDP in D328R $G\alpha_{i1}$ subunits may result in a $G\alpha_i$ subunit exquisitely poised to bind GTP. Similarly, a nucleotide-free $G\alpha_{i1}$ subunit is anticipated to bind to activated receptors with high affinity, and indeed, D328R $G\alpha_{i1}$ subunits display enhanced association with membranes containing activated receptors (Figure 3). This is consistent with the ability of activated receptors to stabilize Gα subunits in the nucleotide-free state. Although $G\alpha_{i1}$ subunits are known to bind to the BODIPY-labeled GTPγS analogue at a slower rate (and with relatively lower affinity) than unlabeled GTPγS (*56*), this reagent provides a useful tool for distinguishing differences in nucleotide exchange between subunits which demonstrate an elevated rate of intrinsic nucleotide exchange.

Peptide binding studies are another tool which can be used to tease out differences among wild-type, D328R, and I56C/Q333C $G\alpha_{i1}$ subunits. The KB-752 peptide which has been shown to bind to the switch II region of inactive $G\alpha_{i1}$ subunits binds to wild-type and D328R $G\alpha_{i1}$ subunits with a similar affinity, not especially surprising given the mutation at residue 328 is in the α5 helix, removed from the switch II region. However, the I56C/Q333C mutation in $G\alpha_{i1}$ subunits does substantially reduce the the level of KB-752 binding, indicating changes in the relative positions of these two helices can be allosterically communicated to the switch II region. On the other hand, both D328R and I56C/Q333C $G\alpha_{i1}$ GDP-AlF_4^- subunits demonstrate a 3−4-fold enhancement in binding affinities for the KB1752 peptide (selective for activated subunits) relative to wild-type $G\alpha_i$. This would be consistent with a conformation for both mutant proteins which favors GDP release and readily adopts the activated conformation, as would be expected for receptor-bound mimetics of activated Gα proteins. However, the differing binding affinities for the mutant subunits to peptides selective for the inactive state, as well as differences in the ability of these proteins to exchange GDP-AlF_4^- for BODIPY-GTPγS, together suggest these mutations exert their effects on nucleotide release through distinct mechanisms.

Mechanisms of GEF-Catalyzed Release of GDP from G Proteins. For small G proteins with soluble GEFs, the GEFs bind across the switch I and switch II regions, and the conformational change induced by this interaction with switch II weakens GDP binding in two ways (*5, 58*). In the case of an Arf-GEF, the Sec7 domain utilizes the carboxylate from a conserved acidic residue of the FG loop of the GEF to form a new hydrogen bond with a lysine in the phosphate-binding P-loop of the G protein, thereby introducing an electrostatic repulsion between the β-phosphate and negatively charged carboxylate group and decreasing nucleotide affinity. Second, the binding of the Mg^{2+} ion in the nucleotide binding pocket is abrogated by steric interference with the

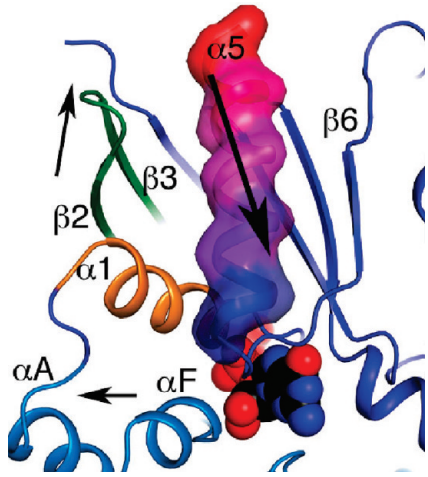

FIGURE 6: Proposed mechanism of receptor-catalyzed GDP release by $G\alpha_{i1}$ mediated by movement of the α5 helix. Crystallographic and biochemical data implicate the receptor-induced movement of the α5 helix toward the bound GDP molecule in destabilization of the guanine ring through Coulombic attraction to the positive helix dipole. The movement of α5 is coupled with a translation in the α1 helix (orange), the $\beta2-\beta3$ hairpin (dark green), and the αF helix (cyan). These concerted motions may be the first step of opening a tunnel to the guanine nucleotide binding pocket and allowing exchange.

new position of switch II. While GPCRs act as GEFs on heterotrimeric G proteins, they do not bind to the switch II region, which is in contact with $G\beta\gamma$. Therefore, a different mechanism appears to have evolved to facilitate nucleotide exchange in Gα subunits. Here, nucleotide exchange is initiated with a roto-translation of the α5 helix, which exerts a Coulombic effect that contributes to a reduction in its GDP binding affinity. While the structure presented here is in complex with GDP-AlF_4^-, there are hints that this Coulombic effect pulls the phosphates of the guanine nucleotide away from the P-loop. Other previously identified structural elements distributed throughout the GTPase domain respond to this roto-translation and nucleotide shift with subtle structural changes (Figure 6 and Movie 1 of the Supporting Information).

The direction of nucleotide egress from the binding site has been debated using terms such as "front door", referring to egress toward the guanine ring, and "back door", referring to egress toward the phosphate corridor (*59*). After the initial roto-translation of the α5 helix, the negatively charged guanine ring may be attracted by a positively charged helix dipole, pulling the base of the guanine nucleotide toward the front door. Such an attraction would likely reorient the nucleotide and weaken the protein−phosphate contacts by pulling the phosphates away from the P-loop. Exit via the front door would require a conformational change in the TCAT motif, the side chain of Arg 176 (on the $\alpha F-\beta2$ loop), and the side chain of Asp 272 (on the α4 helix).

Alternatively, the reorganization of the P-loop and weakened interactions with phosphates may allow nucleotide release through a back door route (Movie 3 of the Supporting Information), with the positively charged dipole shielded from the bound nucleotide through helix capping via negatively charged D328. Exit via the back door requires a change in the position of the main chain of switch II and P-loop regions. Hints about the nature of conformational changes near the back door exit route come from the I56C/Q333C $G\alpha_{i1}$-GDP-AlF_4^- structure. Intriguingly, the position of the switch II region in the I56C/Q333C $G\alpha_{i1}$ structure can be modeled as a continuous motion into the dramatic conformational change observed in the analysis of the complex between the KB-752 and D2N peptides and the $G\alpha_{i1}$ subunit (*31*) (Movie 2 of the Supporting Information). While the KB-752 peptide does not exhibit sequence similarity to Gα binding regions on any known GPCRs, conformational changes of the switch II region upon the binding of KB-752 appear to correlate with increased nucleotide exchange activity in Gα subunits (*50*). In addition to the likely movement of the switch II region during back door nucleotide exchange, the structure of I56C/Q333C $G\alpha_{i1}$ suggests that a subtle shift in phosphate binding residues allows the γ-phosphate binding pocket to adopt a more open position (Figure 4c and Movie 3 of the Supporting Information). A larger conformational change may occur in the P-loop region during physiological GDP release than that seen in the GDP-AlF_4^--bound I56C/Q333C $G\alpha_{i1}$ subunit.

The results presented here do not unambiguously point to exit through either the front or back door, and egress through either route would require a unique arrangement of structural elements of the Gα subunit that has not yet been observed in any published Gα subunit crystal structure. Release of a physiological nucleotide from a front door exit route would likely involve the TCAT motif, $\alpha A-\beta2$ loop, and α4 helix, while a back door egress would likely involve switch II and the P-loop. These data reported here do not discriminate the conformational movements required for GDP egress from those movements that are important for decreasing nucleotide affinity, which is a prerequisite for nucleotide release. If GTP, GTPγS, or GDP-AlF_4^- is bound in the active site, the additional stabilization through protein interactions to the third phosphate (or AlF_4^-) likely prevents the reorientation of the nucleotide, thus blocking the conformational changes that would be required for nucleotide egress. In the absence of the stabilizing influence imparted by a third phosphate or AlF_4^-, GDP-bound subunits may exhibit greater overall conformational flexibility, especially in the switch II and P-loop regions, which are involved in binding AlF_4^- or the γ-phosphate of GTP. The lack of these additional contacts may contribute to allosteric changes at both the front door and the back door of the nucleotide binding site.

The Gα subunit differs from small G proteins in that receptor activation results in association of heterotrimeric $G\alpha\beta\gamma$ with receptors. The $G\beta\gamma$ subunits have been implicated in receptor-mediated nucleotide exchange, and a number of proposals have suggested how these subunits affect GDP release (*31, 60*). While this study cannot address whether $G\beta\gamma$-mediated structural changes follow the initial recognition event between the GPCR and the Gα subunit, the contribution of the roto-translation of the α5 helix to nucleotide exchange does not preclude the involvement of $G\beta\gamma$ in GDP release.

Conclusion. Physiological nucleotide exchange in Gα is likely initiated through a receptor-catalyzed roto-translation of the α5 helix. The data presented here suggest that following receptor binding the change in position of the α5 helix may be transmitted into subtle positional, electrostatic, and dynamic changes throughout Gα that may contribute to the efficiency of G protein activation.

ACKNOWLEDGMENT

Use of the Advanced Photon Source was supported by the U.S. Department of Energy, Office of Science, Office of Basic Energy Sciences, under Contract DE-AC02-06CH11357. Use of IMCA-CAT beamline 17-ID at the Advanced Photon Source was supported by the companies of the Industrial Macromolecular Crystallography Association through a contract with the Center for Advanced Radiation Sources at the University of Chicago. Use of LS-CAT Sector 21 was supported by the Michigan Economic Development Corp. and the Michigan Technology Tri-Corridor for the support of this research program (Grant 085P1000817). We thank G. Liao for expert technical assistance and Eric Dawson for assistance with computer modeling.

SUPPORTING INFORMATION AVAILABLE

Three movies and three figures. This material is available free of charge via the Internet at http://pubs.acs.org.

REFERENCES

1. Oldham, W. M., and Hamm, H. E. (2006) Structural basis of function in heterotrimeric G proteins. *Q. Rev. Biophys. 39*, 117–166.
2. Bourne, H. R. (1997) How receptors talk to trimeric G proteins. *Curr. Opin. Cell Biol. 9*, 134–142.
3. Oldham, W. M., and Hamm, H. E. (2008) Heterotrimeric G protein activation by G-protein-coupled receptors. *Nat. Rev. Mol. Cell Biol. 9*, 60–71.
4. Johnston, C. A., and Siderovski, D. P. (2007) Receptor-mediated activation of heterotrimeric G-proteins: Current structural insights. *Mol. Pharmacol. 72*, 219–230.
5. Vetter, I. R., and Wittinghofer, A. (2001) The guanine nucleotide-binding switch in three dimensions. *Science 294*, 1299–1304.
6. Coleman, D. E., Berghuis, A. M., Lee, E., Linder, M. E., Gilman, A. G., and Sprang, S. R. (1994) Structures of Active Conformations of $G_{i\alpha1}$ and the Mechanism of GTP Hydrolysis. *Science 265*, 1405–1412.
7. Coleman, D. E., and Sprang, S. R. (1998) Crystal Structures of the G Protein $G_{i\alpha1}$ Complexed with GDP and Mg^{2+}: A Crystallographic Titration Experiment. *Biochemistry 37*, 14376–14385.
8. Lambright, D. G., Noel, J. P., Hamm, H. E., and Sigler, P. B. (1994) Structural determinants for activation of the α-subunit of a heterotrimeric G protein. *Nature 369*, 621–628.
9. Mixon, M. B., Lee, E., Coleman, D. E., Berghuis, A. M., Gilman, A. G., and Sprang, S. R. (1995) Tertiary and Quaternary Structural Changes in $G_{i\alpha1}$ Induced by GTP Hydrolysis. *Science 270*, 954–960.
10. Noel, J. P., Hamm, H. E., and Sigler, P. B. (1993) The 2.2 Å crystal structure of transducin-α complexed with GTPγS. *Nature 366*, 654–663.
11. Sondek, J., Lambright, D. G., Noel, J. P., Hamm, H. E., and Sigler, P. B. (1994) GTPase mechanism of G proteins from the 1.7-Å crystal structure of transducin α·GDP·AlF_4^-. *Nature 372*, 276–279.
12. Ferguson, K. M., Higashijima, T., Smigel, M. D., and Gilman, A. G. (1986) The influence of bound GDP on the kinetics of guanine nucleotide binding to G proteins. *J. Biol. Chem. 261*, 7393–7399.
13. Hamm, H. E., Deretic, D., Arendt, A., Hargrave, P. A., Koenig, B., and Hofmann, K. P. (1988) Site of G protein binding to rhodopsin mapped with synthetic peptides from the α subunit. *Science 241*, 832–835.
14. Martin, E. L., Rens-Domiano, S., Schatz, P. J., and Hamm, H. E. (1996) Potent peptide analogues of a G protein receptor-binding region obtained with a combinatorial library. *J. Biol. Chem. 271*, 361–366.
15. Rasenick, M. M., Watanabe, M., Lazarevic, M. B., Hatta, S., and Hamm, H. E. (1994) Synthetic peptides as probes for G protein function. Carboxyl-terminal Gαs peptides mimic Gs and evoke high affinity agonist binding to β-adrenergic receptors. *J. Biol. Chem. 269*, 21519–21525.
16. Cai, K., Itoh, Y., and Khorana, H. G. (2001) Mapping of contact sites in complex formation between transducin and light-activated rhodopsin by covalent crosslinking: Use of a photoactivatable reagent. *Proc. Natl. Acad. Sci. U.S.A. 98*, 4877–4882.
17. Itoh, Y., Cai, K., and Khorana, H. G. (2001) Mapping of contact sites in complex formation between light-activated rhodopsin and transducin by covalent crosslinking: Use of a chemically preactivated reagent. *Proc. Natl. Acad. Sci. U.S.A. 98*, 4883–4887.
18. Nanoff, C., Koppensteiner, R., Yang, Q., Fuerst, E., Ahorn, H., and Freissmuth, M. (2006) The carboxyl terminus of the Gα-subunit is the latch for triggered activation of heterotrimeric G proteins. *Mol. Pharmacol. 69*, 397–405.
19. Denker, B. M., Boutin, P. M., and Neer, E. J. (1995) Interactions between the amino- and carboxyl-terminal regions of Gα subunits: Analysis of mutated Gαo/Gαi2 chimeras. *Biochemistry 34*, 5544–5553.
20. Denker, B. M., Schmidt, C. J., and Neer, E. J. (1992) Promotion of the GTP-liganded state of the Goα protein by deletion of the C terminus. *J. Biol. Chem. 267*, 9998–10002.
21. Kostenis, E., Conklin, B. R., and Wess, J. (1997) Molecular Basis of Receptor/G Protein Coupling Selectivity Studied by Coexpression of Wild Type and Mutant m2 Muscarinic Receptors with Mutant $G\alpha_q$ Subunits. *Biochemistry 36*, 1487–1495.
22. Conklin, B. R., Farfel, Z., Lustig, K. D., Julius, D., and Bourne, H. R. (1993) Substitution of three amino acids switches receptor specificity of $G_q\alpha$ to that of $G_i\alpha$. *Nature 363*, 274–276.
23. Conklin, B. R., Herzmark, P., Ishida, S., Voyno-Yasenetskaya, T. A., Sun, Y., Farfel, Z., and Bourne, H. R. (1996) Carboxyl-Terminal Mutations of $G_{q\alpha}$ and $G_{s\alpha}$ That Alter the Fidelity of Receptor Activation. *Mol. Pharmacol. 50*, 885–890.
24. Blahos, J., Mary, S., Perroy, J., de Colle, C., Brabet, I., Bockaert, J., and Pin, J. P. (1998) Extreme C Terminus of G Protein α-Subunits Contains a Site that Discriminates between G_i-coupled Metabotropic Glutamate Receptors. *J. Biol. Chem. 273*, 25765–25769.
25. Kostenis, E., Gomeza, J., Lerche, C., and Wess, J. (1997) Genetic Analysis of Receptor-$G\alpha_q$ Coupling Selectivity. *J. Biol. Chem. 272*, 23675–23681.
26. Natochin, M., Muradov, K. G., McEntaffer, R. L., and Artemyev, N. O. (2000) Rhodopsin Recognition by Mutant $G_s\alpha$ Containing C-terminal Residues of Transducin. *J. Biol. Chem. 275*, 2669–2675.
27. Ernst, O. P., Meyer, C. K., Marin, E. P., Henklein, P., Fu, W. Y., Sakmar, T. P., and Hofmann, K. P. (2000) Mutation of the Fourth Cytoplasmic Loop of Rhodopsin Affects Binding of Transducin and Peptides Derived from the Carboxyl-terminal Sequences of Transducin α and γ Subunits. *J. Biol. Chem. 275*, 1937–1943.
28. Janz, J. M., and Farrens, D. L. (2004) Rhodopsin Activation Exposes a Key Hydrophobic Binding Site for the Transducin α-Subunit C Terminus. *J. Biol. Chem. 279*, 29767–29773.
29. Scheerer, P., Park, J. H., Hildebrand, P. W., Kim, Y. J., Krauss, N., Choe, H. W., Hofmann, K. P., and Ernst, O. P. (2008) Crystal structure of opsin in its G-protein-interacting conformation. *Nature 455*, 497–502.
30. Onrust, R., Herzmark, P., Chi, P., Garcia, P. D., Lichtarge, O., Kingsley, C., and Bourne, H. R. (1997) Receptor and βγ Binding Sites in the α Subunit of the Retinal G Protein Transducin. *Science 275*, 381–384.
31. Johnston, C. A., and Siderovski, D. P. (2007) Structural basis for nucleotide exchange on Gαi subunits and receptor coupling specificity. *Proc. Natl. Acad. Sci. U.S.A. 104*, 2001–2006.
32. Herrmann, R., Heck, M., Henklein, P., Hofmann, K. P., and Ernst, O. P. (2006) Signal transfer from GPCRs to G proteins: Role of the Gα N-terminal region in rhodopsin-transducin coupling. *J. Biol. Chem. 281*, 30234–30241.
33. Kostenis, E., Zeng, F. Y., and Wess, J. (1998) Functional Characterization of a Series of Mutant G Protein α_q Subunits Displaying Promiscuous Receptor Coupling Properties. *J. Biol. Chem. 273*, 17886–17892.
34. Taylor, J. M., Jacob-Mosier, G. G., Lawton, R. G., Remmers, A. E., and Neubig, R. R. (1994) Binding of an α_2 Adrenergic Receptor Third Intracellular Loop Peptide to Gβ and the Amino Terminus of Gα. *J. Biol. Chem. 269*, 27618–27624.
35. Preininger, A. M., Parello, J., Meier, S. M., Liao, G., and Hamm, H. E. (2008) Receptor-Mediated Changes at the Myristoylated Amino Terminus of Gαi1 Proteins. *Biochemistry 47*, 10281–10293.
36. Lichtarge, O., Bourne, H. R., and Cohen, F. E. (1996) Evolutionarily conserved $G_{\alpha\beta\gamma}$ binding surfaces support a model of the G protein-receptor complex. *Proc. Natl. Acad. Sci. U.S.A. 93*, 7507–7511.

37. Oldham, W. M., Van Eps, N., Preininger, A. M., Hubbell, W. L., and Hamm, H. E. (2006) Mechanism of the receptor-catalyzed activation of heterotrimeric G proteins. *Nat. Struct. Mol. Biol. 13*, 772–777.
38. Marin, E. P., Krishna, A. G., and Sakmar, T. P. (2002) Disruption of the α5 Helix of Transducin Impairs Rhodopsin-Catalyzed Nucleotide Exchange. *Biochemistry 41*, 6988–6994.
39. Medkova, M., Preininger, A. M., Yu, N. J., Hubbell, W. L., and Hamm, H. E. (2002) Conformational Changes in the Amino-Terminal Helix of the G Protein α_{i1} Following Dissociation from G$\beta\gamma$ Subunit and Activation. *Biochemistry 41*, 9962–9972.
40. Dratz, E. A., Furstenau, J. E., Lambert, C. G., Thireault, D. L., Rarick, H., Schepers, T., Pakhlevaniants, S., and Hamm, H. E. (1993) NMR structure of a receptor-bound G-protein peptide. *Nature 363*, 276–281.
41. Otwinowski, Z. (1993) in *CCP4 Study Weekend Data Collection and Processing* (Sawyer, L., Isaacs, N., and Bailey, S., Eds.) pp 56−62, SERC Daresbury Laboratory, Warrington, U.K.
42. Bailey, S. (1994) The CCP4 suite: Programs for protein crystallography. *Acta Crystallogr. D50*, 760–763.
43. McCoy, A. J., Grosse-Kunstleve, R. W., Storoni, L. C., and Read, R. J. (2005) Likelihood-enhanced fast translation functions. *Acta Crystallogr. D61*, 458–464.
44. de la Fortelle, E., and Bricogne, G. (1997) Maximum-likelihood heavy-atom parameter refinement for multiple isomorphus replacement and multiwavelength anomalous diffraction methods. In *Methods in Enzymology. Macromolecular Crystallography Part A* (Carter, C. W., and Sweet, R. M., Eds.) pp 472−494, Academic Press, San Diego.
45. Jones, T. A., Zou, J. Y., Cowan, S. W., and Kjeldgaard, M. (1991) Improved methods for building protein models in electron density maps and the location of errors in these models. *Acta Crystallogr. A47*, 110–119.
46. Brünger, A., Adams, P., Clore, G., DeLano, W., Gros, P., Grosse-Kunstleve, R., Jiang, J., Kuszewski, J., Nilges, M., Pannu, N., Read, R., Rice, L., Simonson, T., and Warren, G. (1998) Crystallography & NMR System: A new software suite for macromolecular structure determination. *Acta Crystallogr. D54*, 905–921.
47. Murshudov, G. N., Vagin, A. A., and Dodson, E. J. (1997) Refinement of macromolecular structures by the maximum likelihood method. *Acta Crystallogr. D53*, 240–255.
48. Adams, P. D., Grosse-Kunstleve, R. W., Hung, L. W., Ioerger, T. R., McCoy, A. J., Moriarty, N. W., Read, R. J., Sacchettini, J. C., Sauter, N. K., and Terwilliger, T. C. (2002) PHENIX: Building new software for automated crystallographic structure determination. *Acta Crystallogr. D58*, 1948–1954.
49. Kleywegt, G. J. (1996) Use of non-crystallographic symmetry in protein structure refinement. *Acta Crystallogr. D52*, 842–857.
50. Johnston, C. A., Willard, F. S., Jezyk, M. R., Fredericks, Z., Bodor, E. T., Jones, M. B., Blaesius, R., Watts, V. J., Harden, T. K., Sondek, J., Ramer, J. K., and Siderovski, D. P. (2005) Structure of $G\alpha_{i1}$ Bound to a GDP-Selective Peptide Provides Insight into Guanine Nucleotide Exchange. *Structure 13*, 1069–1080.
51. Johnston, C. A., Lobanova, E. S., Shavkunov, A. S., Low, J., Ramer, J. K., Blaesius, R., Fredericks, Z., Willard, F. S., Kuhlman, B., Arshavsky, V. Y., and Siderovski, D. P. (2006) Minimal determinants for binding activated Gα from the structure of a Gα(i1)-peptide dimer. *Biochemistry 45*, 11390–11400.
52. Kanaho, Y., Tsai, S. C., Adamik, R., Hewlett, E. L., Moss, J., and Vaughan, M. (1984) Rhodopsin-enhanced GTPase activity of the inhibitory GTP-binding protein of adenylate cyclase. *J. Biol. Chem. 259*, 7378–7381.
53. Van Eps, N., Oldham, W. M., Hamm, H. E., and Hubbell, W. L. (2006) Structural and dynamical changes in an α-subunit of a heterotrimeric G protein along the activation pathway. *Proc. Natl. Acad. Sci. U.S.A. 103*, 16194–16199.
54. Shoemaker, K. R., Kim, P. S., York, E. J., Stewart, J. M., and Baldwin, R. L. (1987) Tests of the helix dipole model for stabilization of α-helices. *Nature 326*, 563–567.
55. Heydorn, A., Ward, R. J., Jorgensen, R., Rosenkilde, M. M., Frimurer, T. M., Milligan, G., and Kostenis, E. (2004) Identification of a Novel Site within G Protein α Subunits Important for Specificity of Receptor-G Protein Interaction. *Mol. Pharmacol. 66*, 250–259.
56. Ramachandran, S., and Cerione, R. A. (2004) Stabilization of an intermediate activation state for transducin by a fluorescent GTP analogue. *Biochemistry 43*, 8778–8786.
57. Abdulaev, N. G., Ngo, T., Ramon, E., Brabazon, D. M., Marino, J. P., and Ridge, K. D. (2006) The receptor-bound "empty pocket" state of the heterotrimeric G-protein α-subunit is conformationally dynamic. *Biochemistry 45*, 12986–12997.
58. Thomas, C., Fricke, I., Scrima, A., Berken, A., and Wittinghofer, A. (2007) Structural evidence for a common intermediate in small G protein-GEF reactions. *Mol. Cell 25*, 141–149.
59. Fisher, A. J., Smith, C. A., Thoden, J., Smith, R., Sutoh, K., Holden, H. M., and Rayment, I. (1995) Structural studies of myosin: nucleotide complexes: A revised model for the molecular basis of muscle contraction. *Biophys. J. 68*, 19S–28S.
60. Rondard, P., Iiri, T., Srinivasan, S., Meng, E., Fujita, T., and Bourne, H. R. (2001) Mutant G protein α subunit activated by G$\beta\gamma$: A model for receptor activation? *Proc. Natl. Acad. Sci. U.S.A. 98*, 6150–6155.

BI801853A